




**Transmission of high-energy electrons through metal-semiconductor Schottky junctions**E. Monteblanco <sup>1,2</sup>, F. Donatini,<sup>1</sup> M. Hehn,<sup>2</sup> D. Lacour <sup>2</sup>, Y. Lassailly,<sup>3</sup> J. Peretti,<sup>3</sup> and N. Rougemaille <sup>1</sup><sup>1</sup>*Univ. Grenoble Alpes, CNRS, Grenoble INP, Institut NEEL, 38000 Grenoble, France*<sup>2</sup>*Institut Jean Lamour, CNRS, Université de Lorraine, BP 70239, 54506 Vandoeuvre lès Nancy, France*<sup>3</sup>*Laboratoire de Physique de la Matière Condensée, Ecole Polytechnique, CNRS, IP Paris, 91128 Palaiseau Cedex, France*

(Received 1 August 2019; published 4 November 2019)

Using the electron beam of a scanning electron microscope as an external current source with tunable energy, we investigate the transport properties of high-energy electrons injected from vacuum into the metal layer of Pt/Cu/Si Schottky junctions. When the injection energy is varied between 1 and 30 keV, the current transmitted into the semiconductor increases by several orders of magnitude and reaches values orders of magnitude larger than the current injected from vacuum. Inspecting the energy dependence of the transmitted current we identify two transport regimes. In the limit of low injection energies and thick metal films, the transport is dominated by the formation and propagation of a secondary electron distribution in the metal layer. However, when the injection energy is sufficiently large and the metal layer sufficiently thin, electrons are transmitted into the semiconductor with negligible energy loss, i.e., the metal layer becomes essentially transparent. The transmitted current is then dominated by impact ionization in the semiconductor. When the metal layer of the Schottky junction is relatively thick and the injection energy of a few keV typically, the transmitted current increases abruptly. The origin of this abrupt change is interpreted as a combined effect of a quasiballistic electron transport in the metal layer and a sudden variation of the density of states in the semiconductor substrate.

DOI: [10.1103/PhysRevB.100.205301](https://doi.org/10.1103/PhysRevB.100.205301)**I. INTRODUCTION**

Metal-semiconductor junctions are often used to study hot electron transport processes as they give access to various physical quantities, such as the Schottky barrier height, the interface transfer coefficients, the electron mean free path in metals or the spin selectivity of ferromagnets. Experimentally, electrons are injected in the metal layer and the current flowing through the Schottky junction is measured. Electron injection can be made in several ways: internal photoemission [1–4], electrical injection [5–10] including local tunneling injection [11–18], or free electron injection from vacuum [19–21]. This latter approach allows controlling the injection energy over a wide range.

Here, we study electron transmission through Pt/Cu/Si junctions for free electron injection energies ranging from 1 to 30 keV. Different regimes are identified in which hot electron transport is dominated either by the secondary electron cascade in the metal and the interface transfer just above the Schottky barrier, or by the ballistic transmission through the metal layer and electron multiplication by impact ionization in the semiconductor. When varying the metal layer thickness, these transport regimes can be probed selectively. A simple model is developed to describe these different processes, which allow estimating the values of the transfer coefficient through the Cu/Si interface, and of the impact ionization threshold in silicon. A close fit of the ballistic transmission measured at high injection energy is obtained when introducing in the model a linear variation with energy of the electron mean free path in the metal [22].

**II. EXPERIMENTAL DETAILS**

The experiments are performed in a scanning electron microscope. The electron beam used for imaging surfaces serves here as an external current source with a tunable energy  $E_0$  (from 1 to 30 keV, typically). *In situ* electrical contacts allow measuring independently the current  $I_B$  flowing in the metal base and the current  $I_C$  collected in the semiconductor. The geometry of the experiment is then similar to a three terminal device [5,7–10] in which the current injection is physically separated from the junction [19–21]. The intensity  $I_0$  of the incoming electron beam is modulated on and off at a typical frequency of 30 Hz, using a beam blanking system. This current modulation thus allows the currents  $I_B$  and  $I_C$  to be measured via a lock-in detection. The current injected into the device ranges from few  $10^2$  pA to few nA, depending on the injection energy and beam conditions. All measurements were performed at room temperature.

The Schottky junctions studied in this work consist of a Pt/Cu bilayer grown on an *n*-doped Si(001) substrate having a resistivity of 1 to 10 Ohm cm. In all samples, the Schottky barrier is ensured by the Cu/Si interface. Prior to the bilayer growth, an ohmic contact was made on the back side of the substrate by depositing an aluminum film subsequently annealed to 400 °C to ensure Al-Si alloying. Then, the native oxide present on the Si wafer was removed and the surface hydrogenated using a cleaning procedure in a HF solution [23]. Finally, the two metals were deposited by magnetron sputtering (base pressure of  $5 \times 10^{-9}$  mbar). After deposition, the samples were patterned into squares using standard

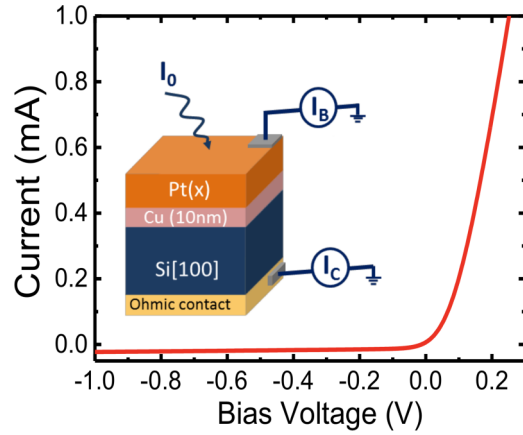


FIG. 1. Typical  $I$ - $V$  curve of a Schottky junction [Pt(100 nm)/Cu(10 nm)/Si(100)]. (Inset) Schematic of the experiment. The Pt/Cu/Si junction is contacted by two independent electrodes, one on the Pt metal layer, allowing the measurement of the current  $I_B$  flowing in the base of the junction, and a second one on the semiconductor substrate, allowing the measurement of the current  $I_C$  flowing in the collector.

UV lithography. The lateral size of the patterned devices is  $870 \mu\text{m}$ . The Schottky junctions were then characterized through conventional current-voltage ( $I$ - $V$ ) measurements (see Fig. 1). The room temperature dynamical resistance  $R_0$  at zero bias, the Schottky barrier height  $\phi_B$ , and the ideality factor  $n$  were deduced from the  $I$ - $V$  curves (see Table I). Overall, these measurements reveal that the Cu/Si contact is similar in all devices, and the values of the junction parameters are compatible with those reported in the literature [1,24–27]. Average values of  $\phi_B = 0.54$  and  $n = 1.07$  can be extracted.

### III. RESULTS

In the following, we define the transmission  $T$  as the ratio of the current  $I_C$  measured in the semiconductor to the current  $I_0$  injected from vacuum (see Fig. 1), which is measured using a Faraday cup. The log-log plot of the transmission measured as a function of  $E_0$  on the five samples is shown in Fig. 2. Consistent with previous works [20,21], the transmission varies over several orders of magnitude and becomes larger than unity (see dashed line in Fig. 2) for injection energies in the keV range. It even reaches values of several  $10^3$  at the highest injection energy we can probe. The collected current is then much larger than the current injected from vacuum, meaning that a multiplication process takes place. This is due to electron-electron scattering which generates supplementary

TABLE I. Characteristics of the Pt/Cu/Si Schottky junctions.

Device	Structure (nm)	$n$	$\phi_B$ (eV)	$R_0$ (k $\Omega$ )
1	Cu(10)/Pt(2)	1.08	0.54	2.9
2	Cu(10)/Pt(10)	1.12	0.51	0.9
3	Cu(10)/Pt(20)	1.03	0.54	3.9
4	Cu(10)/Pt(50)	1.03	0.54	3.3
5	Cu(10)/Pt(100)	1.10	0.55	3.9

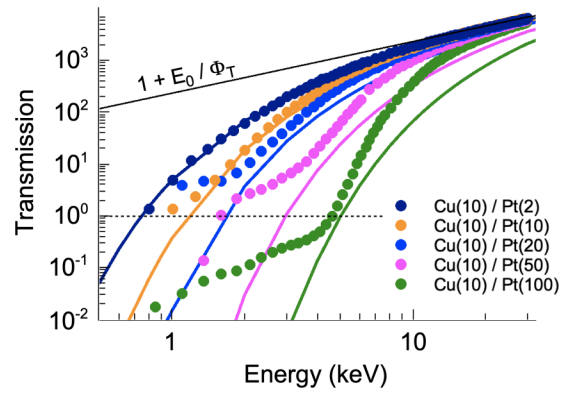


FIG. 2. Transmission as a function of the injection energy  $E_0$  for the five Schottky junctions. Curves are plotted in log-log scales. The dashed line corresponds to a transmission equal to 1. The continuous black line indicates the expected behavior when ballistic transmission through the metal layer and impact ionization in the semiconductor only contribute to the current flowing through the junction. Solid lines are calculated curves after Eq. (2).

carriers in the junction, giving rise to an additional current measured in the semiconductor.

This extra current can be generated either in the metallic base, through a secondary electron cascade [20], or in the semiconductor substrate through impact ionization (i.e., the creation of electron-hole pairs in the Si substrate), providing the electrons enter the semiconductor with an energy larger than the impact ionization threshold [28]. These two processes, schematized in Fig. 3, occur in our experiment.

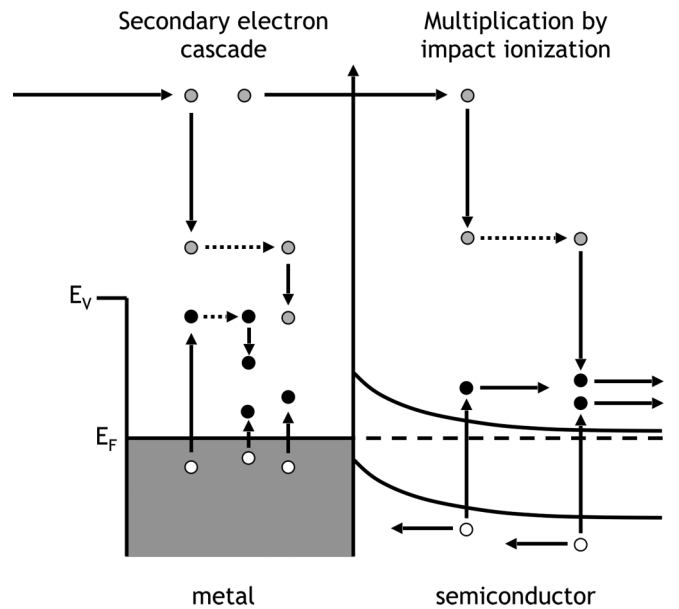


FIG. 3. Schematics of the secondary electron cascade in the metal layer and of the impact ionization mechanism in the semiconductor. Primary electrons are depicted by gray dots, whereas secondary electrons generated in the metal film and in the semiconductor substrate appear as black dots. White dots represent holes.  $E_F$  and  $E_V$  refer to the Fermi and vacuum energies, respectively.

In the high injection energy limit, it is expected that the metal layer becomes transparent to the electrons. In this ballistic transmission regime through the metal layer, electrons enter at high energy in the semiconductor with a high interface transfer efficiency (close to unity). The junction current should thus be fully determined by the impact ionization rate in the semiconductor, and should not depend on the metal layer thickness. This is the reason why all the measured transmission curves in Fig. 2 converge at high injection energy to the same asymptotic linear variation (see black line in Fig. 2).

In the low injection energy range (a few keV, typically), the electron mean free path is much smaller than the metal thickness and the transport is not more dominated by ballistic transmission. In this low-energy regime, the transmission is governed by the secondary electron cascade in the metal layer [20]. This regime is clearly seen on the transmission curves measured on samples with large thicknesses.

At intermediate injection energies (several keV, typically), an abrupt increase in the transmission current is observed for the junctions with the thickest metal layers (see, for example, the green dots in Fig. 2 obtained for device 5). As we will discuss later, this sharp increase in the transmitted current is interpreted as a combined effect of the broadening of the energy distribution of the secondary electrons that forms in the metal layer, and of the increase in the transfer coefficient above the Cu/Si Schottky barrier.

#### IV. TRANSPORT MODELING

In this section, we examine the transport regimes observed experimentally for the different devices to interpret the transmission curves reported in Fig. 2. We assume that the total measured transmission  $T$  is the sum of two terms: a transmission  $T_{\text{ball}}$  originating from the electrons traveling quasiballistically through the metal layer and reaching the semiconductor with negligible energy loss and a transmission  $T_{\text{sec}}$  originating from the secondary electron cascade in the metal. The measured transmission can then be expressed as

$$T = T_{\text{ball}} + T_{\text{sec}}, \quad (1)$$

with both terms being discussed in the following subsections.

##### A. Quasiballistic electron transport in the metal layer and impact ionization in the semiconductor

We first consider the high-energy/low metal thickness regime, in which impact ionization dominates the electron transport. In that regime, we expect the metal layer to be essentially transparent: the incoming electrons are directly transmitted into the semiconductor with negligible energy loss. Once an electron is transmitted into the semiconductor with an energy  $\sim E_0$  higher than the impact ionization threshold energy  $\phi_T$ , electron-hole pairs are excited with an efficiency  $E_0/\phi_T$  [28]. If we note  $\alpha_{HE}$  the transfer coefficient at the Schottky interface, we expect the transmission to vary like

$$T_{\text{ball}} = \alpha_{HE} \left( 1 + \frac{E_0}{\phi_T} \right) \exp(-d/\lambda), \quad (2)$$

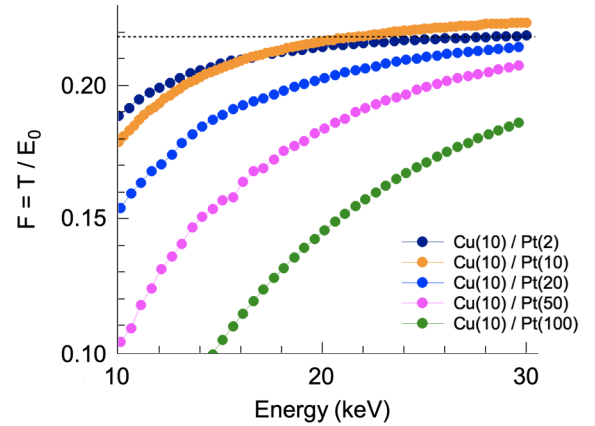


FIG. 4. Energy dependence of the  $F$  functions for the five devices. All curves asymptotically tend to a value of the order of  $0.22 \text{ eV}^{-1}$  (dashed line).

where  $d$  is the thickness of the metal layer and  $\lambda$  the inelastic mean free path (IMFP) at the considered energy. The threshold energy  $\phi_T$  being a constant, and assuming that  $\alpha_{HE}$  is energy independent, the transmission is a linear function of  $E_0$  with a slope  $\alpha_{HE}/\phi_T$  as long as  $d \ll \lambda$ . Otherwise said, the ratio  $F = T/E_0$  should be constant at high injection energy and equal to  $\alpha_{HE}/\phi_T$ . Consistent with this description, we find for the junctions with the thinnest metal layers that  $F \approx 0.22 \text{ eV}^{-1}$  at high injection energies (see Fig. 4). Let us assume that  $\alpha_{HE}$  is close to one, meaning that most of the electrons reaching the Cu/Si interface with a high energy are transmitted into the semiconductor. The value of  $F \approx 0.22 \text{ eV}^{-1}$  thus leads to  $\phi_T \approx 4.5 \text{ eV}^{-1}$ . Taking into account the value of the Schottky barrier height of  $0.54 \text{ eV}$ , we obtain an impact ionization energy of about  $4 \text{ eV}$ , close to the value reported for silicon [29–32]. Considering the simplicity of our transport model, this value, although higher than expected, is in good agreement (within 10%) with former works. In previously reported experiments (and calculations), electrons are directly injected in the semiconductor from vacuum, with a narrow angular distribution, whereas in our experiment electrons undergo scattering in the metal layer, and reach the Schottky interface with a broad wave vector distribution. This broadening of the electron distribution at the interface with the semiconductor may explain the higher value we derive for the impact ionization threshold energy.

We note that  $F$  is constant only for the junctions having a metal thickness of a few tens of nanometers (devices 1 and 2). For these samples, we can thus assume that  $T \approx T_{\text{ball}}$  and use Eq. (2) to fit the experimental transmission curves reported in Fig. 2. The only free parameter remaining in Eq. (2) is the inelastic mean free path  $\lambda$ , which is a function of the injection energy  $E_0$ . In the high energy range we probe in this work,  $\lambda$  can be reasonably assumed to increase linearly with  $E_0$  [22], and since we do not measure the transmission below  $1 \text{ keV}$  typically,  $\lambda$  could be simply expressed as  $aE_0$ , where  $a$  is the only adjustable parameter (see also the Appendix). Based on the measured transmission in the device 1,  $a$  can be estimated to  $\sim 3 \times 10^{-3} \text{ nm eV}^{-1}$ . A very good agreement is then found between Eq. (2) and the transmission measured for the device 1.

However, the best fit is obtained for IMFP values larger than the common values reported in the literature. More specifically, the IMFP we use at 30 keV injection energy is of the order of 90 nm, which is typically three to four times larger than what was reported [22]. This difference is likely due to the fact that we only consider in Eq. (2) a purely ballistic transport, while the distribution of transmitted electrons includes ballistic electrons and quasiballistic electrons that suffered energy losses small compared to  $E_0$ . It is indeed known that electronic excitations like plasmons are efficiently produced by high-energy electrons. However, they lead to energy losses of a few eV typically. Plasmon excitations then contribute to a negligible reduction of the electron IMFP. We thus speculate that, on average, high-energy electrons travel quasiballistically through the metal layer, although they encounter several collisions with energy losses small compared to  $E_0$ . In that case, the incoming electrons can still travel in the metal at high energy across a distance equal to several times the actual IMFP.

### B. Secondary electron cascade in the metal layer

The fit of the transmission curve is in excellent agreement with the measurements done for the Schottky junctions having the thinnest metal layer (device 1 and device 2), suggesting that a ballistic transport in the metal, followed by an electron multiplication through impact ionization in the semiconductor, describes well our experimental findings. As expected, the quality of the fit degrades as the metal thickness of the junction is increased. For example, although the fit seems to capture the abrupt change of the transmission, it fails at providing the correct shape and value of the transmission for thick metal layers. This is particularly visible for device 5. We interpret this result as a consequence of a change in the transport mechanism as the metal thickness is increased. For the junctions with the thinnest metal layers, the metal film is almost transparent, meaning that the IMFP in the metal at high energy is large enough so that the current generated by the ballistic transmission dominates. This approximation is not valid anymore for thicker metal films, and the formation of a secondary electron distribution in the metal layer that propagates at a much smaller energy must be considered. We thus argue that we observe experimentally a change in the transport regime, from a transport dominated by a quasiballistic regime for the thinnest metal layers to a regime dominated by secondary electrons for thicker metal films.

For the devices with a thick metal layer, we can isolate the dominant contribution  $T_{\text{sec}}$  of the secondary electrons generated in the metal. In Fig. 5 we have plotted the variation of  $T_{\text{sec}} = T - T_{\text{ball}}$  obtained from the measured transmission curve on device 5 and from the calculated contribution of the ballistic transmission with Eq. (2). For the calculation of  $T_{\text{ball}}$ , we have used the values of the parameters  $a$  and  $\phi_T$  deduced in the previous section from the analysis of the transmission measured on device 1. The obtained variation of  $T_{\text{sec}}$  exhibits two transmission regimes: a slowly varying signal at low energy followed by an abrupt increase above 4 keV. Following the ideas developed in a previous work [20],

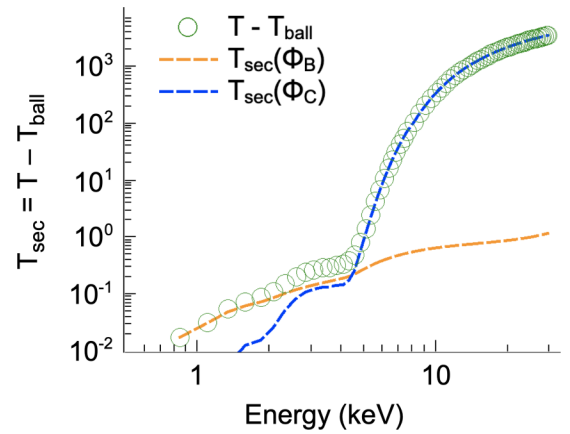


FIG. 5. Transmission of secondary electrons ( $T_{\text{sec}}$ ) deduced from the measurements performed on device 5 (green open circles). Orange and blue dashed lines represent, respectively, the two contributions  $T_{\text{sec}}(\phi_B)$  and  $T_{\text{sec}}(\phi_C)$  deduced from Eqs. (5) and (6), and the estimate of the energy  $E_M$ .

we define the transmission as

$$T_{\text{sec}} = [1 - \exp(-d/\lambda)]M \int_0^{+\infty} \alpha(\epsilon)f(\epsilon)d\epsilon, \quad (3)$$

where  $M = E_0/E_M$  is the multiplication factor related to the secondary electron cascade in the metal layer. This factor is nothing else than the energy conservation: the energy  $E_0$  of a primary electron is shared between  $M$  electrons (the primary and the secondary electrons) having a mean energy  $E_M$ . The function  $f(\epsilon)$  is the normalized electron distribution reaching the Cu/Si interface and  $\alpha(\epsilon)$  is the transfer coefficient through the Schottky interface for electrons of energy  $\epsilon$  (averaged over the wave vector distribution of the secondary electrons reaching the interface).

The increase in the electron multiplication coefficient  $M$  with increasing  $E_0$  contributes to the increase in  $T$ . However, this cannot explain the abrupt change observed at high injection energy in the variation of  $T_{\text{sec}}$  (see Fig. 5). This change is in fact due to the conjunction of two factors: the broadening of the secondary electron distribution at the Cu/Si interface and the increase of the  $\alpha(\epsilon)$  value above  $\phi_B$ .

The broadening of the secondary electron distribution at the Cu/Si interface is due to the increase with  $E_0$  of the electron mean free path in the metal layer. Let us take for the secondary electron distribution an exponential function  $f(\epsilon) = E_M^{-1} \exp(-\epsilon/E_M)$  (see Refs. [19,20,33]), where  $E_M$  is the mean energy of the electron distribution reaching the Cu/Si interface. Here,  $E_M$  is supposed to be small compared to  $\phi_T$  (i.e., impact ionization is neglected, although it can be taken into account in Eq. (3) for electrons transmitted above  $\phi_C$  in the high energy tail of the secondary electron distribution [28]). This choice for  $f(\epsilon)$  is somehow arbitrary and is mainly intended to ease the calculation. However, it reflects the fact that in the low-energy regime the electron distribution at the Schottky interface is “thermalized” as the number of electron-electron collisions is high (the IMFP in this regime is much smaller than the metal thickness). Then, when  $E_0$  increases, the broadening of the secondary electron distribution is simply described by the increase of  $E_M$ .



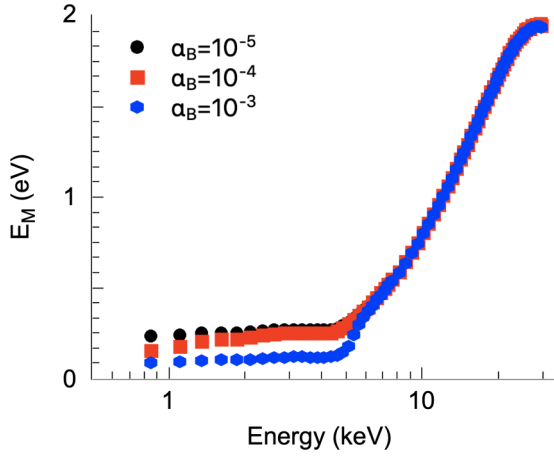


FIG. 6. Mean energy of the electron distribution at the Cu/Si interface for the device 5 calculated from Eq. (4) and using the experimental data points from which we subtracted the contribution  $T_{\text{ball}}$ .  $E_M$  is calculated for different  $\alpha_B$  values. Black dots, red rectangles, and blue hexagons correspond to  $\alpha_B$  values of  $10^{-5}$ ,  $10^{-4}$ , and  $10^{-3}$ , respectively.

The interface transfer function  $\alpha(\epsilon)$  is equal to zero if  $E_M < \phi_B$  (no leakage current below the Schottky barrier). Then,  $\alpha(\epsilon)$  increases above  $\phi_B$ , due to the increase with energy  $\epsilon$  of the available density of states in Si, and of the wave vector acceptance at the interface [34]. Let us consider that  $\alpha(\epsilon)$  exhibits a steplike variation:  $\alpha(\epsilon)$  is equal to a constant  $\alpha_B$  above  $\phi_B$ , and is equal to  $\alpha_{HE} = 1$  above an energy  $\phi_C$ , which is related to the electronic structure of the metal-semiconductor interface. It is indeed known that  $\alpha(\epsilon)$  may increase step by step by several orders of magnitude for  $\epsilon$  values coinciding either to different valleys of the semiconductor conduction band [9] or to the barrier of an interface oxide layer [16,20]. In previous works,  $\alpha_B$  was found to be of the order of  $10^{-4}$  [8–10,13,20]. We chose here this value, while we assume that  $\phi_C$  corresponds to the edge of the conduction band at the Brillouin zone center. We thus take  $\phi_C = 2.9$  eV above the Fermi level (when taking into account the Schottky barrier height). However, as we will see below, the precise variation of  $\alpha(\epsilon)$  (as long as it increases monotonously and reaches a value close to unity a few eV above  $\phi_B$ ) does not change significantly the energy dependence of the electron transmission.

The transmission can then be expressed as [20,28]

$$T_{\text{sec}} = [1 - \exp(-d/\lambda)] \frac{E_0}{E_M} [\alpha_B \exp(-\phi_B/E_M) + (\alpha_{HE} - \alpha_B) \exp(-\phi_C/E_M)]. \quad (4)$$

This expression of the transmission can be used to estimate  $E_M$  from the measurements [20,28]. To do so, we use the experimental data points reported in Fig. 5, which correspond to the sole contribution of the secondary electrons to the transmission. Then, Eq. (4) is solved to obtain  $E_M$  [35]. The energy dependence of  $E_M$  is plotted in Fig. 6 in linear-log scales. For the device 5, we find that  $E_M$  is of the order of 100 meV at low injection energy and stiffly increases above  $\approx 4$  keV. This is the expected behavior when considering the increase with the energy of the electron IMFP in the metal [20].

Note that the same treatment can be done for different values of the  $\alpha_B$  constant, and the deduced variation of  $E_M$  is only weakly affected by  $\alpha_B$  (see Fig. 6). Instead of taking a step-by-step variation of  $\alpha(\epsilon)$ , we have also performed the same analysis using a linear variation from zero to 1 between  $\phi_B$  and  $\phi_C$ . In this case  $E_M$  takes lower values but exhibits a similar variation versus  $E_0$ : small and almost constant at low injection energy and stiffly increasing above  $\approx 4$  keV.

The variation of  $E_M$  can then be reinjected in Eq. (4) to separate the two contributions to the transmission of the secondary electrons crossing the interface above  $\phi_B$  with the transfer coefficient  $\alpha_B$ , and above  $\phi_C$  with the transfer coefficient  $\alpha_{HE}$ :

$$T_{\text{sec}}(\phi_B) = [1 - \exp(-d/\lambda)] \alpha_B \frac{E_0}{E_M} \times [\exp(-\phi_B/E_M) - \exp(-\phi_C/E_M)] \quad (5)$$

and

$$T_{\text{sec}}(\phi_C) = [1 - \exp(-d/\lambda)] \alpha_{HE} \frac{E_0}{E_M} \exp(-\phi_C/E_M). \quad (6)$$

These two contributions to the transmission are plotted in Fig. 5 in orange and blue dashed lines. At low injection energy,  $E_M$  is small and transmitted electrons have an energy close to  $\phi_B$  for which the interface transfer efficiency is small. At high injection energy, the secondary electron distribution broadens, i.e.,  $E_M$  increases, and the transmission is dominated by electrons of energy larger than  $\phi_C$  which are transferred through the Cu/Si interface with an efficiency close to unity. The transition between the two transport regimes depends on the metal layer thickness. For thinner metal layer, the transition occurs for smaller  $E_0$  values when the secondary electron multiplication factor is smaller. For higher  $E_0$  values, the contribution of the secondary electron multiplication is overwhelmed by the contribution of the ballistic transmission and the multiplication by impact ionization in silicon. This latter transmission regime is not observed in thick metal layer in the probed energy range but should arise at higher injection energy, providing the electron mean free path becomes larger than the metal layer thickness.

## V. SUMMARY

High-energy electrons were injected from vacuum into Pt/Cu/Si Schottky junctions having similar properties but different metal thicknesses. For injection energies ranging from 1 to 30 keV, we find that the current transmitted into the semiconductor increases by several orders of magnitude and reaches values  $10^3$  times larger than the incoming current, due to carrier multiplication processes. Using a simple model to describe the energy dependence of the transmission, we identified two main transport regimes: a quasiballistic electron transport in the limit of high injection energies and thin metal layers and a secondary electron cascade in the limit of low injection energies and thick metal films. From the analysis of these different transport regimes, we gain physical insight on the electron distribution reaching the Cu/Si interface. Finally, we provide here an easy-to-implement method for investigating hot electron transport across metal-semiconductor interfaces. In particular, the use of the free electron beam

provided by a scanning electron microscope is well suited for controlling the injection energy in a wide range.

### ACKNOWLEDGMENTS

This work was supported by the Agence Nationale de la Recherche through Project No. ANR-16-CE09-0025 ‘‘POLARSPIN’’.

### APPENDIX: ENERGY DEPENDENCE OF THE INELASTIC MEAN FREE PATH

The only free parameter in the expression of  $T_{\text{ball}}$  [Eq. (2)] is the inelastic mean free path  $\lambda$  (IMFP) that we defined as  $\lambda = aE_0$ , where  $a$  is a constant. This constant is chosen to best fit the transmission measured for the junction having the thinnest metal layer (device 1). We then find that  $a = 3.1 \times 10^{-3} \text{ nm eV}^{-1}$ , leading to  $\lambda = 93 \text{ nm}$  at 30 keV. However, we fixed the linear dependence of  $\lambda$  with  $E_0$ , although we could have chosen otherwise. For example, Seah and Hunt suggested a square root variation of  $\lambda$  with  $E_0$  [36], while Tanuma *et al.* proposed an energy dependence close to  $E_0^{0.8}$  [22]. We have thus also fitted the transmission curves with several power laws. The results are reported in Fig. 7 for the devices 1 and 5, and for three energy dependences. In all cases, the  $a$  constant is chosen in such a way that  $\lambda = 93 \text{ nm}$  at 30 keV. Best fits are clearly obtained for a linear dependence of  $\lambda$  with the energy, whereas the two other fits poorly describe our experimental findings. Given the approximations we made to describe the quasiballistic transport in the metal layer and the carrier multiplication associated with impact ionization in the semiconductor, our fits provide the energy dependence of the IMFP.

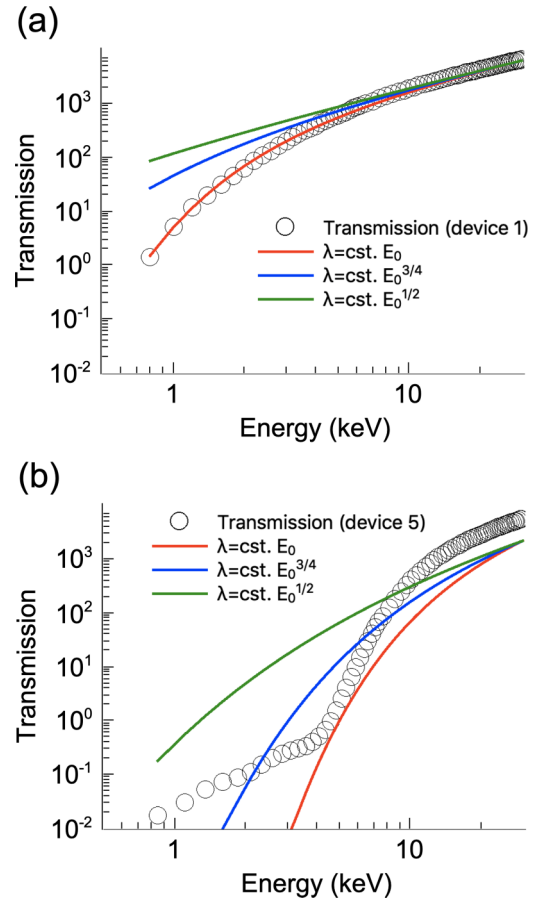


FIG. 7. Fits of the transmission curves for different energy dependences of the IMFP. (a) Device 1. (b) Device 5.

- [1] C. R. Crowell, W. G. Spitzer, L. E. Howarth, and E. E. LaBate, *Phys. Rev.* **127**, 2006 (1962).
- [2] S. M. Sze, J. L. Moll, and T. Sugano, *Solid-State Electron.* **7**, 509 (1964).
- [3] E. H. Rhoderick, in *Metal-Semiconductor Contacts*, edited by P. Hammond and D. Walsh (Oxford University, Oxford, 1978).
- [4] J. Peretti, H.-J. Drouhin, and D. Paget, *Phys. Rev. B* **47**, 3603 (1993).
- [5] J. P. Spratt, R. F. Schwarz, and W. M. Kane, *Phys. Rev. Lett.* **6**, 341 (1961).
- [6] G. Spitzer, C. R. Crowell, and M. M. Atalla, *Phys. Rev. Lett.* **8**, 57 (1962).
- [7] D. J. Monsma, J. C. Lodder, T. J. A. Popma, and B. Dieny, *Phys. Rev. Lett.* **74**, 5260 (1995).
- [8] S. van Dijken, X. Jiang, and S. S. P. Parkin, *Phys. Rev. B* **66**, 094417 (2002).
- [9] S. van Dijken, X. Jiang, and S. S. P. Parkin, *Phys. Rev. Lett.* **90**, 197203 (2003).
- [10] S. van Dijken, X. Jiang, and S. S. P. Parkin, *J. Appl. Phys.* **97**, 043712 (2005).
- [11] W. J. Kaiser and L. D. Bell, *Phys. Rev. Lett.* **60**, 1406 (1988).
- [12] L. D. Bell and W. J. Kaiser, *Phys. Rev. Lett.* **61**, 2368 (1988).
- [13] W. H. Rippard and R. A. Buhrman, *Phys. Rev. Lett.* **84**, 971 (2000).
- [14] A. Thiaville, F. Caud, C. Vouille, and J. Miltat, *Eur. Phys. J. B* **55**, 29 (2007).
- [15] A. Kaidatzis, S. Rohart, A. Thiaville, and J. Miltat, *Phys. Rev. B* **78**, 174426 (2008).
- [16] S. Guézo, P. Turban, C. Lallaizon, J. C. Le Breton, P. Schieffer, B. Lépine, and G. Jézéquel, *Appl. Phys. Lett.* **93**, 172116 (2008).
- [17] S. Guézo, P. Turban, S. Di Matteo, P. Schieffer, S. Le Gall, B. Lépine, C. Lallaizon, and G. Jézéquel, *Phys. Rev. B* **81**, 085319 (2010).
- [18] M. Hervé, S. Tricot, S. Guézo, G. Delhaye, B. Lépine, P. Schieffer, and P. Turban, *J. Appl. Phys.* **113**, 233909 (2013).
- [19] A. Filipe, H.-J. Drouhin, G. Lampel, Y. Lassailly, J. Nagle, J. Peretti, V. I. Safarov, and A. Schuhl, *Phys. Rev. Lett.* **80**, 2425 (1998).
- [20] N. Rougemaille, D. Lamine, G. Lampel, Y. Lassailly, and J. Peretti, *Phys. Rev. B* **77**, 094409 (2008).
- [21] X. Li, E. Tereshchenko, S. Majee, G. Lampel, Y. Lassailly, D. Paget, and J. Peretti, *Appl. Phys. Lett.* **105**, 052402 (2014).

- [22] S. Tanuma, C. J. Powell, and D. R. Penn, *Surf. Interface Anal.* **43**, 689 (2011).
- [23] C. Vautrin, Y. Lu, S. Robert, G. Sala, O. Lenoble, S. Petit-Watelot, X. Devaux, F. Montaigne, D. Lacour, and M. Hehn, *J. Phys. D: Appl. Phys.* **49**, 355003 (2016).
- [24] T. Arizumi and M. Hirose, *Jpn. J. Appl. Phys.* **8**, 749 (1969).
- [25] M. O. Aboelfotoh, *J. Appl. Phys.* **69**, 3351 (1991).
- [26] M. O. Aboelfotoh and B. G. Svensson, *Semicond. Sci. Technol.* **6**, 647 (1991).
- [27] R. Balsano, A. Matsubayashi, and V. P. LaBella, *AIP Adv.* **3**, 112110 (2013).
- [28] D. Lamine, Ph.D. thesis, Ecole Polytechnique, Palaiseau, France, 2008, <https://tel.archives-ouvertes.fr/tel-00260976>.
- [29] C. Bussolati, A. Fiorentini, and G. Fabri, *Phys. Rev.* **136**, A1756 (1964).
- [30] F. E. Emery and T. A. Rabson, *Phys. Rev.* **140**, A2089 (1965).
- [31] C. A. Klein, *J. Appl. Phys.* **39**, 2029 (1968).
- [32] J. Fang, M. Reaz, S. L. Weeden-Wright, R. D. Schrimpf, R. A. Reed, R. A. Weller, M. V. Fischetti, and S. T. Pantelides, *IEEE Trans. Nucl. Sci.* **66**, 444 (2019).
- [33] A. van der Sluijs, Ph.D. thesis, Ecole Polytechnique, 1996.
- [34] This effect is probably reinforced in silicon because of the indirect nature of the band gap. Indeed, at low energy, conduction states are only available near the Brillouin zone edge.
- [35] To deduce  $E_M$  from Eq. (4) we neglected the contribution of  $\alpha_B$  in the second term as  $\alpha_B \ll \alpha_{HE}$ . We also neglected the influence of the  $1 - \exp(-d/\lambda)$  prefactor since it is close to one for realistic IMFP in the whole energy range we probe in this work.
- [36] M. P. Seah and C. P. Hunt, *Surf. Interface Anal.* **5**, 33 (1983).